V European Conference on Computational Fluid Dynamics
ECCOMAS CFD 2010
J. C. F. Pereira and A. Sequeira (Eds)
Lisbon, Portugal, 14–17 June 2010

# PREDICTION OF SHOCK STRUCTURE BY BIMODAL DISTRIBUTION FUNCTION METHOD

**Maxim A. Solovchuk**[*], **Tony W. H. Sheu**[*,†]

[*] Department of Engineering Science and Ocean Engineering, National Taiwan University,
No. 1, Sec. 4, Roosevelt Road, Taipei, Taiwan 10617, Republic of China
e-mail: solovchuk@gmail.com

[††] Center for Quantum Science and Engineering (CQSE), National Taiwan University
e-mail: twhsheu@ntu.edu.tw

**Key words:** fluid dynamics, shock wave, kinetic theory

**Abstract.** *A system of fluid dynamic equations is derived by using Mott-Smith distribution function to study the structure of shock wave in a neutral, monatomic gas of Maxwell molecules. The predicted shock solutions using the newly proposed formalism are presented and compared with the experimental data, direct-simulation Monte Carlo (DSMC) solution and the solutions predicted by other existing theories for Mach numbers M<10. The density, temperature, heat flux profiles and shock thickness calculated at different Mach numbers have been shown to have good agreement with the experimental and DSMC solutions. In addition, the predicted shock thickness is in good agreement with the DSMC simulation result at low Mach numbers.*

## 1 INTRODUCTION

Normal shock wave is an example of highly non-equilibrium flow. An important parameter describing the non-equilibrium properties of the gas is Knudsen number, which can be defined in a shock wave as a relation between the mean free path and shock thickness. In the shock wave macroscopic properties of the gas change very rapid within a short distance, which is about several mean free paths and the Knudsen number becomes large.

The shock wave structure can not be described well by fluid dynamic equations in the sense that Navier-Stokes equations [1] give good agreement with the experimental data [2] only at Mach numbers M<1.3. Burnett, super Burnett and their modification [3] improved the results, but their theories can be only applied to the cases with Mach numbers $M \le 3$. When applying the Burnett and super Burnett equations some non-physical oscillations were found to appear in the solution even at M=2. In Grad method and extended irreversible thermodynamics [4] a large number of equations must be solved to get a reasonable accuracy. Grad's 13-moment method was succeeded to simulate shock profile below the critical value $M_C$=1.65. In [5] it was mentioned that one needs up to 680 moments (64 one-dimensional equations) to calculate a smooth shock structure for M=1.8 that fits well to the experimental data. In case of strong shocks the Knudsen number becomes large. With the increasing number of moments in extended thermodynamics [4] the solution converges rather slowly. Therefore, a large number of moments is required to describe the processes at large Knudsen numbers.

Good agreement with the experimental measurements was obtained on the basis of bimodal distribution function [6]. Mott-Smith pointed out that the distribution function in a strong shock wave is bimodal and can be expressed by $f = a(x) f_0 + (1 - a(x)) f_1$, where $f_0$ and $f_1$ are the local-equilibrium distribution functions for describing the supersonic and subsonic flows and a(x) is the unknown quantity. Because of its simplicity and correct prediction of shock thickness at large Mach numbers it was applied to several shock formation problems, including the shock structure in dense gases and gas mixtures, relativistic shocks, plasma problem [6-9]. However, there exist several nontrivial deficiencies in this theory [9]. The first drawback is that there is no unique way that is currently available to determine the unknown quantity a(x), which needs to be determined from a moment equation given by the Boltzmann equation. The choice of velocity moment, while it can be arbitrary, can greatly affect the predicted result in the sense that the computed shock thickness can be different by an amount of 25% [6]. Bashkirov and Orlov [10] used nonanalitical moments in velocity space and their results can have a difference about 80-100%. As a result, a better procedure should be adopted. The second deficiency is attributed to the incorrect prediction of shock thickness at low Mach numbers.

The Mott-Smith method gives a reasonable agreement with the experimental data and the Monte-Carlo simulation result for strong shocks [11]. As a result, we use the Mott-Smith distribution function in this paper to derive six fluid dynamic equations in one-dimensional domain. By virtue of the system of fluid dynamic equations, the problem of choosing an appropriate velocity moment will be automatically resolved. Use of a system of six equations instead of four equations in Mott-Smith method allows us to get rid of the incorrect shock structure prediction at low Mach numbers and gives us some additional information about the behaviors of temperature, heat flux, pressure in the whole range of Mach numbers. We will use the collision integral for Maxwell molecules [12]. For the case of real particle interaction potential, we will take the temperature dependent viscosity into account.

## 2 FLUID DYNAMICS EQUATIONS

The kinetic equation in one-dimensional case takes the following form

$$\frac{\partial f}{\partial t}+V_X\frac{\partial f}{\partial x}=J^B \tag{1}$$

where $f$ is the distribution function of a gas, $t$ the time, and $J^B$ the integral of collisions. In this study we will consider the case of Maxwell molecules. The following subset of basic functions is used:

$$\varphi_1=m,\varphi_2=mV_X,\varphi_3=m\xi^2/2,$$
$$\varphi_4=\frac{m}{2}\xi_X{}^2,\varphi_5=\frac{m}{2}\xi_X\xi^2,\varphi_6=\frac{m}{2}\xi_X{}^3 \tag{2}$$

In the above, $\vec{\xi}=\vec{V}-\vec{U}$ represents the peculiar velocity and $\vec{U}=(U,0,0)$ is the stream velocity.

Let us define a scalar product in velocity space as follows:

$$<\varphi_I,f>\equiv\ <\varphi_I>=\int d\vec{V}\varphi_I f$$

The moments of distribution function are related to the thermodynamic variables as follows:

$$\rho=<\varphi_1>,\rho U=<\varphi_2>,\frac{3\rho}{2m}kT=<\varphi_3>,$$
$$P_{XX}=<\varphi_4>,q_X=<\varphi_5>,\bar{q}_X=<\varphi_6>. \tag{3}$$

Here $m$ denotes the mass of a molecule, $k$ the Boltzmann constant, $\rho$ the mass density, T the temperature, $P_{XX}$ the diagonal component of pressure tensor, $q_X$ the vertical component of heat flow, and $\bar{q}_X$ the new parameter having a dimension as the heat flow.

One can project the kinetic equation (1) on the velocity moments (2) to get the following system of fluid dynamic equations:

$$\begin{aligned}
&\frac{\partial}{\partial t}\rho+\frac{\partial}{\partial x}(\rho U)=0\\
&\frac{\partial}{\partial t}U+U\frac{\partial}{\partial x}U+\frac{1}{\rho}\frac{\partial}{\partial x}P_{xx}=0\\
&\frac{3k}{2m}\frac{\partial}{\partial t}(\rho T)+\frac{3k}{2m}U\frac{\partial}{\partial x}(\rho T)+(\frac{3k}{2m}\rho T+P_{xx})\frac{\partial}{\partial x}U+\frac{\partial}{\partial x}q_x=0\\
&\frac{\partial}{\partial t}P_{xx}+U\frac{\partial}{\partial x}P_{xx}+3P_{xx}\frac{\partial}{\partial x}U+2\frac{\partial}{\partial x}\bar{q}_x=-\frac{p}{\mu}(P_{xx}-\frac{\rho}{m}kT)\\
&\frac{\partial}{\partial t}q_x+U\frac{\partial}{\partial x}q_x+2(q_x+\bar{q}_x)\frac{\partial}{\partial x}U-(\frac{3k}{2m}T+\frac{1}{\rho}P_{xx})\frac{\partial}{\partial x}P_{xx}+\frac{\partial}{\partial x}J_1=-\frac{2}{3}\frac{p}{\mu}q_x\\
&\frac{\partial}{\partial t}\bar{q}_x+U\frac{\partial}{\partial x}\bar{q}_x+4\bar{q}_x\frac{\partial}{\partial x}U-\frac{3}{2\rho}P_{xx}\frac{\partial}{\partial x}P_{xx}+\frac{\partial}{\partial x}J_2=-\frac{p}{\mu}(\frac{3}{2}\bar{q}_x-\frac{1}{2}q_x)
\end{aligned} \tag{4}$$

where $p$ denotes the pressure and $\mu$ is the viscosity. The above system of equations contains $J_1$ and $J_2$, which are given by

$$J_1=\int d\vec{V}\xi_x{}^2\xi^2 f\ ,\ J_2=\int d\vec{V}\xi_x{}^4 f=<\xi_x{}^4> \tag{5}$$

To close the above system of equations in Eq. (4), we have to prescribe the distribution function. In Refs. [13] and [14] the problem of wave disturbance propagation was studied in a rarefied gas within the context of the above system. To

close the system of differential equations in Eq. (4), a piecewise continuous distribution function was used. The agreement with experimental data was good for the phase velocity at all Knudsen numbers. In this study we will choose the bimodal distribution function [6], one describing the subsonic and the other accounting for the supersonic flow:

$$f = f_0 + f_1 \tag{6}$$

where

$$f_0 = n_0(x)\left(\frac{m}{2\pi k T_0}\right)^{3/2} \exp\left(-\frac{m(\vec{V}-\vec{U}_0)^2}{2kT_0}\right) \tag{7}$$

and similarly for $f_1$ with the subscript 0 being replaced by the subscript 1 throughout. The parameters $T_0, T_1, \vec{U}_1 = (U_1, 0, 0)$, $\vec{U}_0 = (U_0, 0, 0)$ are assumed to be independent of *x* and *t*. We'll introduce them in the next section through the Rankine-Hugoniot relations. According to the definitions of density and velocity in (3), we can get the following two expressions through the employed distribution function

$$n_0(x) = n(x)\frac{(U_1 - U(x))}{(U_1 - U_0)},$$

$$n_1(x) = n(x)\frac{(U(x) - U_0)}{(U_1 - U_0)}.$$

The expressions of the integrals $J_{1,2}$ shown in Eq. (5) are given below

$$\begin{aligned} J_1 &= \frac{n_0(x)}{2}(U-U_0)^4 + 2(U-U_0)^2 n_0(x) {V_{T0}}^2 + \frac{5}{8} n_0(x) {V_{T0}}^4 \\ &+ \frac{n_1(x)}{2}(U-U_1)^4 + 2(U-U_1)^2 n_1(x) {V_{T1}}^2 + \frac{5}{8} n_1(x) {V_{T1}}^4, \\ J_2 &= \frac{n_0(x)}{2}(U-U_0)^4 + \frac{3}{2}(U-U_0)^2 n_0(x) {V_{T0}}^2 + \frac{3}{8} n_0(x) {V_{T0}}^4 \\ &+ \frac{n_1(x)}{2}(U-U_1)^4 + \frac{3}{2}(U-U_1)^2 n_1(x) {V_{T1}}^2 + \frac{3}{8} n_1(x) {V_{T1}}^4 \end{aligned} \tag{8}$$

where ${V_T}^2 = 2kT/m$.

## 3 SHOCK STRUCTURE

The shock wave, which is stationary in the steady frame of reference under current investigation, connects the equilibrium states of density $\rho_0$, velocity $U_0$ and temperature $T_0$ ahead of the shock at $x \to -\infty$ and the equilibrium quantities $\rho_1, U_1, T_1$ behind the shock at $x \to \infty$. It is convenient to use the dimensionless equations for system (4), where the upstream values are used to define the following dimensionless quantities:

$$\begin{aligned} &\rho' = \frac{\rho}{\rho_0}, U' = \frac{U}{\sqrt{kT_0/m}}, T' = \frac{T}{T_0}, x' = \frac{x}{\lambda_0}, \\ &\pi' = \frac{\pi}{k\rho_0 T_0/m}, q' = \frac{q}{\rho_0 (kT_0/m)^{3/2}} \end{aligned} \tag{9}$$

where $\pi = p_{xx} - \rho kT/m$ and $\lambda_0$ is the mean free path. The mean free path given in Refs. [2,3,12] will be adopted in this study

$$\lambda_0 = \frac{16}{5\sqrt{2\pi}} \frac{\mu_0}{\rho_0 \sqrt{k/mT_0}} \approx \frac{1}{0.783} \frac{\mu_0}{\rho_0 \sqrt{k/mT_0}} \tag{10}$$

The first three equations, cast in their dimensionless forms, in the differential system (4) are as follows:

$$\begin{aligned} &\frac{d}{dx}(\rho U) = 0 \\ &\frac{d}{dx}(\rho U^2 + \rho T + \pi) = 0 \\ &\frac{d}{dx}(\frac{1}{2}\rho U^3 + \frac{5}{2}\rho T U + \pi U + q) = 0 \end{aligned} \tag{11}$$

Far ahead of and behind the shock the gas is in equilibrium with $\pi_0 = \pi_1 = 0$ and $q_0 = q_1 = 0$. The dimensionless quantities before the shock at $x \to -\infty$ are given by:

$$T_0 = 1,\ \rho_0 = 1,\ U_0 = \sqrt{\frac{5}{3}} M_0 \tag{12}$$

Integration of all equations in Eq. (11) between the two equilibrium states gives:

$$\begin{aligned} &\rho_1 = \frac{4M_0^{\,2}}{M_0^{\,2} + 3} \\ &U_1 = \sqrt{\frac{5}{3}} \frac{M_0^{\,2} + 3}{4M_0} \\ &T_1 = \frac{(5M_0^{\,2} - 1)(M_0^{\,2} + 3)}{16M_0^{\,2}} \end{aligned} \tag{13}$$

It is worth noting that use of the above equations, which are well known as the Rankine-Hugoniot relations, enables us to prescribe the boundary conditions.

The number of equations can be reduced further by integrating equations in Eq. (11) from the upstream state to an arbitrary location *x* in the shock. By taking into account Eq. (12), we get:

$$\begin{aligned} &\rho U = \rho_0 U_0 \\ &\rho U^2 + \rho T + \pi = \rho_0 U_0^{\,2} + \rho_0 T_0 \\ &\frac{\rho U^3}{2} + \frac{5}{2}\rho T U + \pi U + q = \frac{\rho_0 U_0^{\,3}}{2} + \frac{5}{2}\rho_0 T_0 U_0 \end{aligned} \tag{14}$$

The following relations can be obtained by solving the above three equations in (14):

$$\begin{aligned} &\rho(U) = \sqrt{\frac{5}{3}} \frac{M_0}{U} \\ &\pi(U,T) = 1 + \frac{5}{3} M_0^{\,2} - \sqrt{\frac{5}{3}} M_0 (\frac{T}{U} + U) \\ &q(U,T) = \sqrt{\frac{5}{12}} M_0 (\frac{5}{3} M_0^{\,2} + 5 + U^2 - 3T) - U(1 + \frac{5}{3} M_0^{\,2}) \end{aligned} \tag{15}$$

Then we substitute the relations in Eq. (15) into the differential system (4) to get the following system of three coupled ordinary differential equations for governing the transport of velocity *U*, temperature *T* and $\overline{q}$ below:

$$A\begin{pmatrix}\frac{d}{dx}U\\ \frac{d}{dx}T\\ \frac{d}{dx}\bar{q}\end{pmatrix}=-\frac{p\lambda_0}{\mu\sqrt{kT_0/m}}\begin{pmatrix}G_1(U,T,\bar{q})\\ G_2(U,T,\bar{q})\\ G_3(U,T,\bar{q})\end{pmatrix} \tag{16}$$

where $A$ is the 3*3 matrix with the nonlinear components. The boundary conditions for the investigated system are specified as

$$T_0=1,\ U_0=\sqrt{\frac{5}{3}}M_0,\bar{q}_0=0 \text{ at } x\to-\infty \tag{17}$$

At $x\to\infty$, we impose

$$U_1=\sqrt{\frac{5}{3}}\frac{{M_0}^2+3}{4M_0},\ T_1=\frac{(5{M_0}^2-1)({M_0}^2+3)}{16{M_0}^2},\ \bar{q}_1=0 \tag{18}$$

The system of equations was derived on the basis of Gross-Jackson model of Boltzmann equation that corresponds to the special case of Maxwell molecules. The corresponding viscosity is proportional to the temperature following the expression given below with s=1:

$$\mu=\mu_0\left(\frac{T}{T_0}\right)^s \tag{19}$$

It is well known that the viscosity also takes this form for other interaction potentials just with an adjustment of the exponent *s* [2,11,12]. In particular, s =1/2 is chosen for hard sphere and s ≈ 0.72 for argon [2,15]. Other authors [15] advised to use the value s ≈ 0.68. We will, as a result, use these two values to see which of them agrees better with experiment. According to Eqs. (10) and (19), one gets

$$\frac{\nu\lambda_0}{\sqrt{kT_0/m}}=\frac{\rho T^{1-S}}{0.783} \tag{20}$$

## 4 COMPARISON STUDY AND DISCUSSION OF RESULTS

To predict the temperature and velocity in shock profiles from the proposed system of ordinary differential equations in Eq. (16), subjected to boundary conditions (17) and (18), the computational domain is descretized into N+2 positions $x_i$ with $i=0,1,2...,N+1$ and step size $\Delta x$. The following approximation is used at the node $i$:

$$\left.\frac{dT}{dx}\right|_i=\frac{T_{i+1}-T_{i-1}}{2\Delta x}$$

Calculation of the solutions at positions $x_1$ and $x_N$ requires to know the field values at $x_0$ and $x_{N+1}$, which are given by (17), (18). So we can derive 3N coupled algebraic equations for the N unknown values for *U*, *T* and $\bar{q}$. The resulting nonlinear system was solved with the appropriate $\tanh(x)$ curve being considered as an initial guess for the velocity and temperature (similar to [3]). The predicted temperature and density are presented in a normalized form:

$$\frac{T-T_0}{T_1-T_0},\frac{n-n_0}{n_1-n_0}$$

One of the main parameters which can well describe the shape of shock profile is the shock thickness. The shock thickness is defined as

$$\delta = \frac{\rho_1 - \rho_0}{\max(\frac{\partial \rho}{\partial x})}$$

The inverse thickness can be derived from Eq. (21) as $\frac{\lambda}{\delta} = \frac{\alpha}{4}$ according the Mott-Smith theory. Another quantity is the temperature-density separation $\Delta_{T\rho}$, which is defined as the distance between the middle point of temperature and density.

In Fig. 1 we compare the results of this work with the results of other authors for the inverse density thickness. For weak shocks the agreement between our results and Monte-Carlo simulation [16] is excellent. Mott-Smith theory [6] predicts a relatively larger thickness at low Mach numbers.

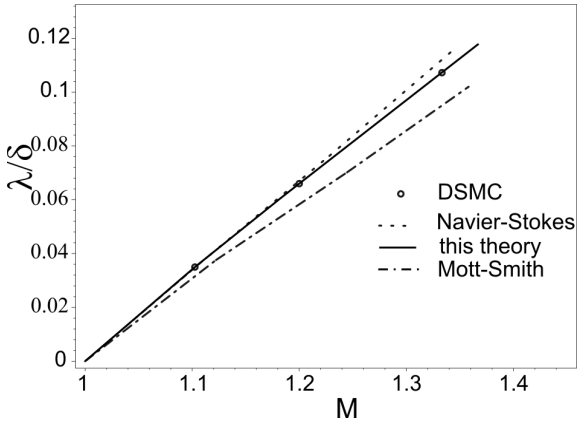


Figure 1: Comparison of the predicted inverse density thicknesses against the Mach number. The results of this paper are compared with those based on different theories: Navier-Stokes [1], Mott-Smith [6], DSMC[16].

The predicted values of the temperature-density separation $\Delta_{T\rho}$ shown for Maxwell molecules in Fig. 2 are compared well with the Monte-Carlo simulations [16], Mott-Smith theory [6] and Navier-Stokes results [1]. Our results are in good agreement with the DSMC calculation in the range of Mach numbers 1<M<2.5. The predicted Navier-Stokes solution is correct only at M<1.3 and the solution calculated by Mott-Smith theory gives a good agreement with the DSMC values simply at 2.2<M<2.5.

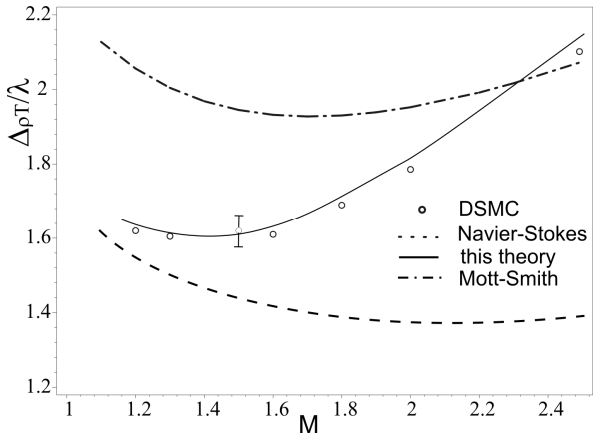


Figure 2: The plot of the predicted temperature-density separation against the Mach number. Notation – see Fig. 1.

In Figs. 3-4 we compare our results for the heat flux profiles with DSMC simulation results [17] for Maxwell molecules, Navier-Stokes results and Mott-Smith results at Mach numbers M=1.7, 10. Heat flux is a higher moment of the distribution function and the difference between theories is clearly seen. The normalized density of our solutions is exactly 0.5 at the coordinate origin x=0 at any Mach number. Navier-Stokes solutions fail to describe shock profiles at Mach numbers M>1.7. At M=1.7 the predicted heat flux of Mott-Smith theory is larger than the Nanbu DSMC simulation values. At M>3 Mott-Smith prediction of heat flux lies below the DSMC simulation results. Our results agree well with the DSMC simulation for the heat flux profile.

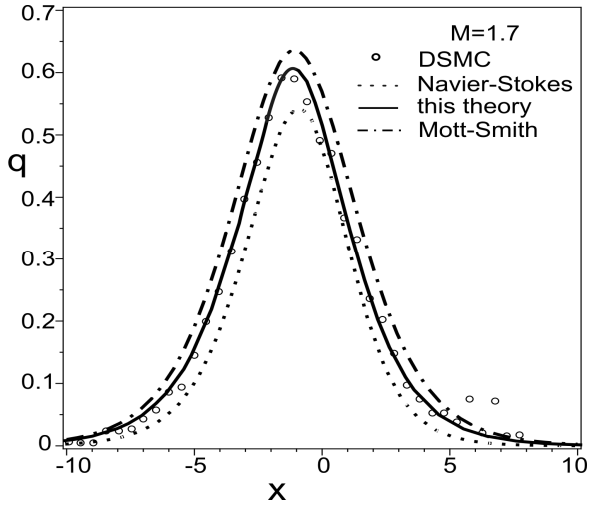


Figure 3: Comparison of the heat flux profiles plotted as a function of the distance. Comparison of the currently simulated results with the DSMC simulation results [17], Navier-Stokes [1] and Mott-Smith [6] results at M=1.7.

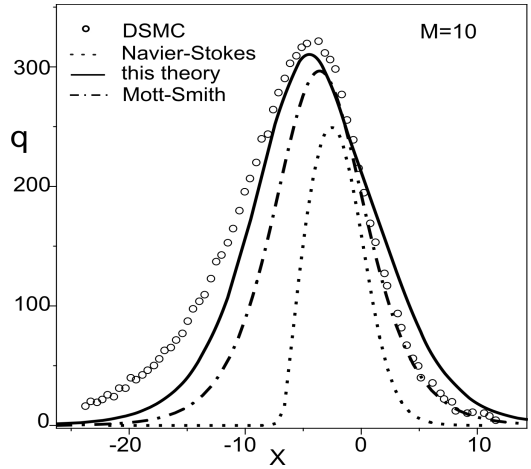


Figure 4: Comparison of the heat flux profiles plotted as a function of the distance at M=10.

The temperature profile in Fig. 5 shows its maximum within the shock layer, which can't be predicted by Mott-Smith theory and Navier-Stokes equations. The temperature profile becomes nonmonotonic at a Mach numbers M>3. It is well known that such a predicted temperature profile is not a mathematical artifact but is rather the result of atomistic dynamics. In this article we use six fluid dynamic equations, while Mott-Smith used four equations. We can see that the increasing number of equations helps us to improve the prediction of shock profile.

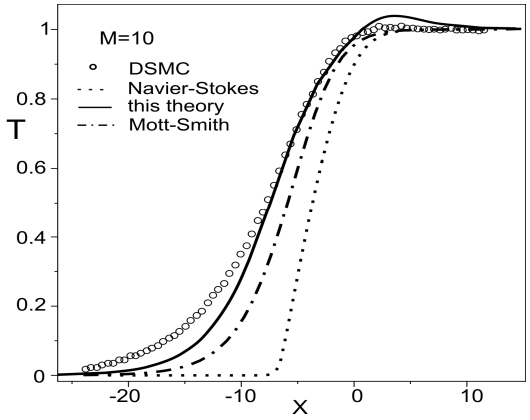


Figure 5.Comparison of the predicted temperature profiles at M=10.
Notation – see Fig. 3. Note that temperature shows an overshot.

It is worth noting that the predicted temperature-density separation is smaller for the Mott-Smith theory than DSMC value. The temperature-density separation by Mott-Smith theory $\Delta_{T\rho} = 5.89\lambda_0$ at M=10, while in our theory $\Delta_{T\rho} = 7.44\lambda_0$ which agrees with DSMC value [17]. For the Navier-Stokes equations we got the value $\Delta_{T\rho} = 3.68\lambda_0$. In Fig. 6 the predicted values of temperature-density separation are compared with the Monte-Carlo simulation results [17]. Our results agree well with DSMC calculation in the range of Mach numbers 1<M<10. Mott-Smith theory gives good agreement with DSMC simulation only in the range of Mach numbers 2.2<M<2.7.

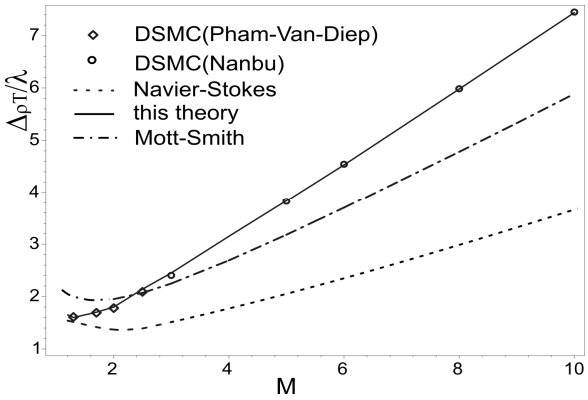


Figure 6. The plot of the predicted temperature-density separation against the Mach number.
Diamonds – DSMC results of Pham-Van-Diep [16], circles-DSMC results of Nanbu [17].

In Fig. 7 the results computed from the derived system are compared with the measurements of the inverse shock thickness for argon [2]. The values *s=0.72* and *s=0.68* chosen for the viscosity exponent yield a good agreement with the experimental data. We estimate that *s=0.70* would provide the best agreement with experimental data.

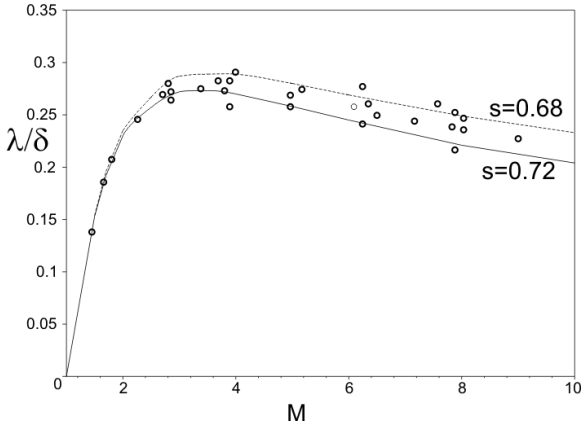


Figure 7. Comparison of the predicted inverse density thicknesses with the experimental data – circles.

## 5 CONCLUSION

A system of fluid dynamic equations was derived on the basis of Mott-Smith distribution function for the Maxwell molecules. On the basis of the derived system, the structure of shock wave in a neutral monatomic gas was studied. The predicted shock thickness is seen to have a good agreement with the Monte-Carlo simulation at all Mach numbers. The predicted inverse density thickness for Argon is also in good agreement with experimental data. In contrast to the Mott-Smith theory, the derived system predicts correct shock thickness, temperature-density separation and correct shock profile at a low Mach number. The Mott-Smith solution is qualitatively correct for M=2~3. At other Mach numbers their predicted errors are large. Our predicted temperature and heat flux profiles agree well with the Monte-Carlo simulation in the investigated range of Mach numbers $1.7<M<10$. In extended thermodynamics, many moments are required in order to get a predicted solution with good agreement with the experimental result. With the Mott-Smith closure, a fairly good agreement with the experimental and the Monte-Carlo simulation results can be obtained even from a differential system with much fewer equations. The proposed procedure can be applied for the further development of processes in polyatomic gases, gas mixtures, plasma and problem in astrophysics.

## REFERENCES

[1] D. Gilbarg and D. Paolucci, The structure of shock waves in the continuum theory of fluids. *J. Rat. Mech. Anal* **2**, pp. 617-642 (1953)

[2] H. Alsmeyer, Density profiles in argon and nitrogen shock waves measured by the absorption of an electron beam, *J. Fluid Mech*. **74**, pp. 497-513 (1976)

[3] M. Torrilhon, H. Struchtrup, Regularized 13 moment equations: shock structure calculations and comparison to Burnett models, *J. Fluid Mech*. **513**, pp. 171-198 (2004)

[4] I. Muller and T. Ruggeri, Rational Extended Thermodynamics (Springer, New York, 1998)

[5] J. D. Au, Nichtlineare Probleme and Losungen in der Erweiterten Thermodynamik. Ph.D. Thesis, Technical University Berlin 2000

[6] H. M. Mott-Smith, The solution of the Boltzmann equation for a shock wave. *Phys. Rev.* **82**, pp. 885-892 (1951)

[7] J. Pruet, Neutrinos from the propagation of a relativistic jet through a star. *Astrophys. J*. **591**, pp. 1104-1109 (2003).

[8] S. Mazouffre, P. Vankan, R. Engeln, and D. C. Schram, Behavior of the H atom velocity distribution function within the shock wave of a hydrogen plasma jet. *Phys. Rev. E* **64**, pp. 066405-1-8 (2001).

[9] I N Ivchenko, S K Loyalka, R V Tompson Jr, Analytical Methods for Problems of Molecular Transport (Fluid Mechanics and Its Applications) Springer 2007

[10] A. G. Bashkirov and A. V. Orlov. Shock-wave structure for some nonanalytical in-velocity closures. *Phys. Rev. E* **53**, pp. R17-R20 (1996).

[11] G. A. Bird, Molecular Gas Dynamics and the Direct Simulation of Gas Flows. Oxford University Press, New York, (1994)

[12] T. Chapman and T. G. Cowling. The Mathematical Theory of Non-uniform Gases (Cambridge University Press, Cambridge, 1970).

[13] D. A. Vereshchagin, S. B. Leble, M. A. Solovchuk. Piecewise continuous distribution function method in the theory of wave disturbances of inhomogeneous gas. *Phys. Lett. A* **348**, pp. 326-334 (2006)

[14] S. Leble, M. Solovchuk, "One-dimensional ultrasound propagation in stratified gas," *Archives of Acoustics* **34**(2), pp. 215-229 (2009)

[15] C. J. Greenshields and J. M. Reese. The structure of shock waves as a test of Brenner's modifications to the Navier–Stokes equations. *J. Fluid Mech.* **580**, pp. 407-429 (2007).

[16] G. C. Pham-Van-Diep, D. A. Erwin, and E. P. Muntz. Testing continuum descriptions of low-Mach-number shock structures. *J. Fluid Mech.* **232**, pp. 403-413 (1991)

[17] K. Nanbu and Y. Watanabe, Analysis of the internal structure of shock waves by means of the exact direct-simulation method, *Report of the Institute of High Speed Mechanics*, Tohoku University, Japan, Vol. 48, 1984.